

A 6 DOF TESTING MACHINE CONTROLLED BY DIGITAL IMAGE CORRELATION: AN EXPERIMENTAL SETUP FOR NEW NOORU-MOHAMED TESTS

**M. PONCELET*, J. LE FLOHIC*†, V. PARPOIL*,
 H. LECLERC*, B. RAKA*, AND J.-M. VIRELY***

*LMT Cachan

ENS Cachan/CNRS/UPMC/PRES UniverSud Paris
 61 av. du Président Wilson, 94235 Cachan Cedex, France
 e-mail: poncelet@lmt.ens-cachan.fr, www.lmt.ens-cachan.fr

†Now at Institut Pascal

UMR 6602 UBP/CNRS/IFMA

Campus de Clermont-Ferrand - Les Cézeaux BP 265 - 27 rue Roche Genes, 63175 AUBIERE Cedex, France
 e-mail: Julien.Le-Flohic@ifma.fr, http://ip.univ-bpclermont.fr/

Key words: Nooru-Mohamed Test, Concret, Digital Image Correlation, Stewart Platform, Hexapod

Abstract. A new experimental setup for concrete mixed-mode crack propagation is presented. The specimen and loading correspond to a Nooru-mohamed test, *i.e.* a square double-notched specimen submitted to in-plane tension and shear. Innovation comes from the loading setup: a hexapod machine whose 3D motions are controlled by a Digital Images Correlation algorithms using several cameras “live” recordings. The interest of this setup is that the 3D (in-plane and out-of-plane) boundary conditions will be controlled contrary to the original Nooru-Mohamed setup, which conditions have a tremendous influence on the crack propagation, and thus further confrontations to numerical simulations.

1 INTRODUCTION

The Nooru-Mohamed (NM) tests, schematically shown on figure 1, consist in submitting a double notched concrete specimen to a combination of shear and tension loading. They are characterized by complex mixed-mode crack propagation, and are therefore interesting for model validations, and extensively used for this purpose. Unfortunately, according to Nooru-Mohamed himself [1], boundary conditions of the tests were not well known. Moreover, at the time of these experiments, full-field measurements were only burgeoning and were not used by Nooru-Mohamed, even though NM tests are intrinsically heterogeneous. The aim of this work is thus to both reproduce NM results and

improve NM tests with today rich, trustworthy and versatile experimental techniques to help model validation.

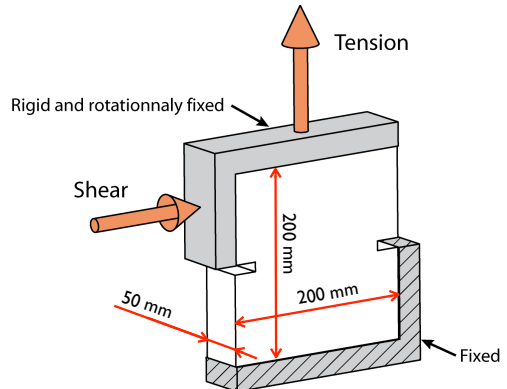


Figure 1: Principle of Nooru-Mohamed test.

Performing a NM test is an experimental challenge for several reasons. First, the specimen is very stiff, quasi-fragile with a low elastic limit. Second, the applied load is multiaxial (tension and shear) and not aligned (shear). Last, theoretical loading is in-plane, and small out-of-plane loading may tremendously change the crack behaviour. Consequently one has to accurately measure and control very small displacements (around 10 to 20 μm at the onset of failure) and strains whereas the applied load is high (around 10 to 20 kN at the onset of failure), inducing deformation of the loading system and potential spurious effects, such as out-of-plane loading.

This proceeding presents a new experimental setup, based on a highly multiaxial testing machine (an hexapod) controlled with a dedicated Integrated Digital Image Correlation (IDIC) algorithm. The main interest of the proposed technique is its low measurement uncertainty in comparison with more standard techniques of vision-based machine control. Last one are generally using marker tracking which is very fast, but less accurate. First, we will briefly explain the principle of the setup. Second, we will focus on the IDIC algorithm with its mathematical formulation and numerical implementation. Last, a presentation of the first results of measurement will be shown. We will conclude on the expected control performance and future NM test possibilities.

2 PRINCIPLE OF THE SETUP

2.1 Loading machine

The first key point of this modern version of NM experiments is to perform tests using a Stewart platform (a.k.a. hexapod). Very few tests have already been performed with such type of machine. To the authors knowledge, the only examples are a biomechanical test of a spine joint [3] and a series of test concerning composite material [4]. The specimen is glued to the two ends of the machine; namely a still lower platform and the moving upper one (figure 2). Feasibility of such an experiment has already been proved by the authors [2] in

the case of a simple displacement law (two in-plane loadings: tension and shear). This type of machine offers 6 degrees of freedom (DOF) (3 translations + 3 rotations) whereas during a standard NM test, only two in-plane loadings are used (tension and shear). The extra DOF will enable to control as much as possible boundary conditions, *i.e.* correct potential unwanted motions (in-plane rotation, out-of-plane bending and translation).

Because such machine is rather flexible, the use of the joints measurements, in this case the actuator lengths, doesn't enable a reliable displacement control.

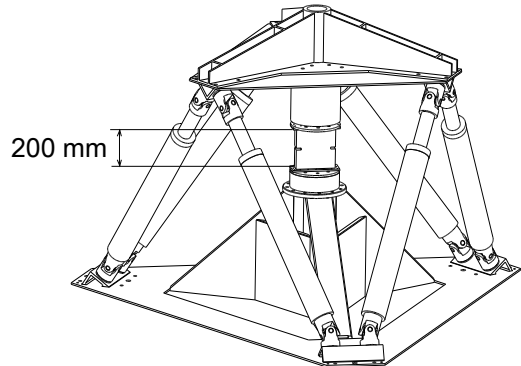


Figure 2: Scheme of the hexapod in a Nooru-mohamed test configuration.

2.2 Measurement and control setup

Consequently, the second key point is to perform the control by directly measuring the relative displacement of the two ends of the testing machine. To this aim, several cameras will be fastened to the lower end of the machine, each aiming at a “target” fastened to the upper end of the machine. The measurement, achieved through an Integrated Digital Image Correlation (IDIC) technique, will be incorporated in the feedback control loop. Technically speaking, one will not measure the complete 3D rigid body motion and then relate it to the 6 DOF of the hexapod, but directly measure the “equivalent” actuator lengths, *i.e.* taking into account the stiffness of the entire machine. To this aim a calibration matrix C_i relating 3D Rigid Body

Motion to actuators displacement has to be determined before measurement.

The Figure 3 shows the principle of the whole setup with the different units :

- The control unit, where hexapod position command is generated, converted into actuator length by the kinematic model, compared to the measure and introduced in the PID corrector. These calculations are very simple and don't limit the frequency of the overall control loop.
- The hexapod, driven by the actuator lengths calculated by the PID. The hexapod has its own inner control loop embedded in the drive controllers. A new command can be received every 4 ms. Previous command is maintained until a new one is received.
- The cameras, with their own acquisition frequency. The frequency has to be chosen depending on the velocity of the command. They are automatically started so that the delay between the images of each camera is negligible in comparison to the period of acquisition.
- The IDIC unit, where the measure is obtained by an iterative solving of the global problem including the latest image of all the used cameras at each inner iteration. To have a very low computation time of the each inner iteration, GPU implementation is used. This way, convergence is reached and the measure is sent to the control unit before a new set of images is received. A more detailed explanation of the IDIC algorithm is given in the next section.

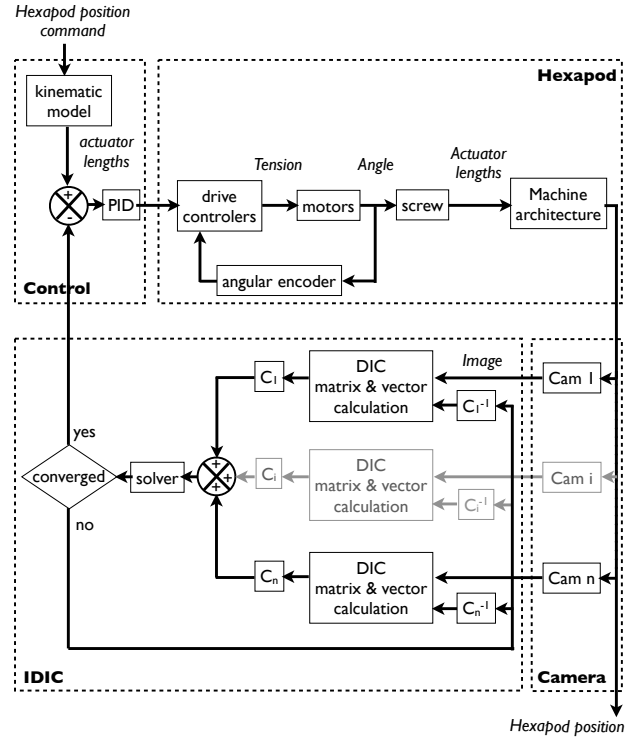


Figure 3: Principle of the control setup.

3 IDIC ALGORITHM

3.1 Integrated Digital Image Correlation principle

In a DIC algorithm, an initial image f is related to a deformed image g , the displacement field \underline{u} , and the camera noise n by Eq. 1.

$$g(\underline{x} + \underline{u}) = f(\underline{x}) + n(\underline{x}) \quad . \quad (1)$$

Solving the problem, *i.e.* measuring \underline{u} , consists in minimizing a functional Φ over a set of possible displacements \underline{v}

$$\Phi(\underline{v}) = \iint (g(\underline{x} + \underline{v}) - f(\underline{x}))^2 d\underline{x} \quad . \quad (2)$$

The set of displacements \underline{v} is chosen in a space of 6 shape functions that corresponds to rigid body motions, denoted by $\varphi_i(\underline{x})$

$$\underline{v}(\underline{x}) = \sum_{i=1}^6 v_i \cdot \underline{\varphi}_i(\underline{x}) \quad . \quad (3)$$

Shape functions are used to prescribe the displacements of the nodes of a mesh. In our case, the mesh only contains one element that covers

the whole image (integrated DIC), to enhance computation time without missing one of the sought displacements.

Under the small perturbation assumption and by minimizing the functional over the v_i , we obtain a set of 6 equations

$$\begin{aligned} \forall j \in [1, 6], \\ \sum_{i=1}^7 \iint (\underline{\varphi}_i(\underline{x}) \cdot \underline{\nabla} g(\underline{x})) \cdot (\underline{\varphi}_j(\underline{x}) \cdot \underline{\nabla} g(\underline{x})) d\underline{x} \cdot v_i \\ = \iint (f(x) - g(x)) \underline{\varphi}_j \cdot \underline{\nabla} g d\underline{x} \quad (4) \end{aligned}$$

which could be written using a matrix $[M]$ and a vector \underline{F} in the following way

$$[M] \cdot \underline{v} = \underline{F} \quad . \quad (5)$$

Usually, the quantity of interest is \underline{v} , the measured displacement over the basis of shape functions. This system is usually solved iteratively. In this case, another approach has been used to suppress the use of the kinematic model during measurement and avoid using the exact position of the cameras.

A strong hypothesis has been made: we assume a linear relation between the displacement measured by a camera over the set of shape functions (\underline{u}) and the 6 actuator lengths (\underline{L}_a). This linear relation is determined by a calibration step : each actuator is moved independently and the displacement measured by each camera is saved in a “calibration matrix” $[C]$. We then get the relation $\underline{u} = [C] \cdot \underline{L}_a$, that we use in Eq. 5 in order to measure the actuator lengths. This calibration step is made before a test, while the machine is ready for a test, but without a specimen and unloaded.

Theoretically, this measurement of \underline{L}_a could be made using only one camera. However the uncertainty over the out-of-plane motions obtained using the algorithm is then too high to control the hexapod in the case of “sensitive” tests such as NM one. Indeed, the uncertainty of rotation R_x or R_y corresponds to a lateral displacement of the sample of about $250\mu\text{m}$, *i.e.* far more than the displacement at failure. Considering the geometry of the machine, it is wise

to use at least two, or even better, three cameras. We then denote the number of cameras by k .

There is one linear system by camera, as written in Eq. 6.

$$\forall i \in [1, k], \quad [M_i] \cdot [C_i] \cdot \underline{L}_a = \underline{F}_i \quad . \quad (6)$$

To make the solving of such systems possible, we multiply it by $[C_i]^{-1}$ (Eq. 7).

$$\forall i \in [1, k], \quad [C_i]^{-1} \cdot [M_i] \cdot [C_i] \cdot \underline{L}_a = [C_i]^{-1} \cdot \underline{F}_i \quad . \quad (7)$$

We then add the systems together (Eq. 8) to obtain an unique system which solution is the actuators length. It produces a natural weighting in between the components of the different $[M_i]$ and F_i

$$\left(\sum_{i=1}^k [C_i]^{-1} \cdot [M_i] \cdot [C_i] \right) \cdot \underline{L}_a = \sum_{i=1}^k [C_i]^{-1} \cdot \underline{F}_i \quad . \quad (8)$$

One can denote that this development could be adapted to another type of testing machine, and is not dependent of the number of cameras.

3.2 Numerical implementation

A specific program is in charge of starting camera’s acquisition, performing DIC computations, controlling the hexapod, displaying user interface. For the sake of responsiveness, stability and permanence, it has been developed in C++. The UI is a webpage that could be displayed remotely. Using object oriented programming, the integration of such different tasks has been possible.

The challenge of the software implementation is the computation loop that needs to be quick, below 50 ms. The use of Graphical Processing Units (GPUs) to perform quick DIC computation has already been demonstrated by the authors [5] and has been integrated in this software.

The DIC computation are realized on different GPUs using separate threads. Each iteration gives $[M]$ and \underline{F} for each camera. After each iteration, the threads are synchronized and hold, so that we can introduce the actuators length (\underline{L}_a) and calibration matrices ($[C_i]$) as described by Eqs. 6 and 7. The systems are added (Eq. 8),

and the actuator length is determined by solving the global system (Eq. 9).

$$\underline{L}_a = \left(\sum_{i=1}^k [C_i]^{-1} \cdot [M_i] \cdot [C_i] \right)^{-1} \cdot \sum_{i=1}^k [C_i]^{-1} \cdot \underline{F}_i \quad (9)$$

To deform pictures and to compute the next iteration, we need to use the actuator length measured to obtain the displacement seen by each camera over the shape function's space (\underline{u}_i). This is done by using the “calibration relation” $\underline{u}_i = [C_i] \cdot \underline{L}_a$. Then, the different DIC threads can continue separately from these new results.

4 FIRST APPLICATION AND RESULTS

4.1 Experimental setup

The loading machine is a Bosch-Rexroth hexapod (Figure 4) previously used for truck driving simulation. Each actuator has a theoretical resolution of displacement of $0,15 \mu\text{m}$ and a load capacity of 25 kN. The present hexapod architecture allows for a workspace about 500^3 mm^3 , with very interesting mechanical features summarized in Table 1. x and y stand for horizontal axes (x is perpendicular to one side of the base triangle), z is the vertical axis. (x,y,z) a right-hand orientation. For further details and application to a NM test, see [2].

Table 1: Mechanical features of the hexapod, given for actuators at mid-length.

	x	y	z
Force capacity (kN)	57	54	125
Torque capacity (kN.m)	46	41	71
Translation resolution (μm)	3,95	0,54	0,19

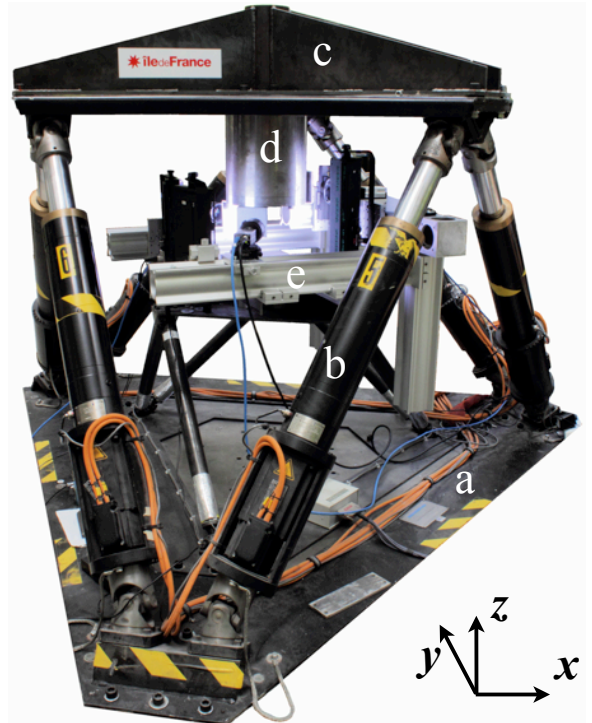


Figure 4: Hexapod: (a) base, (b) actuator, (c) moving upper end, (d) shaft of the upper end, (e) still lower end with optical setup.

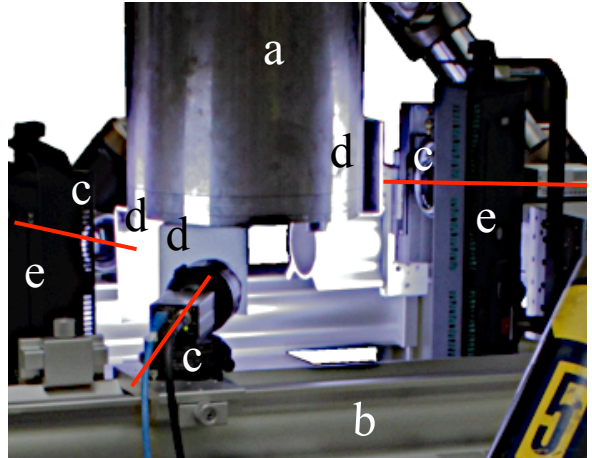


Figure 5: Optical setup: (a) shaft of the upper end, (b) lower end with optical rails, (c) cameras, (d) “targets”, (e) lights. Optical axes are marked with red lines.

For this first test, 3 cameras are clamped to the lower part of the machine, aiming at 3 targets fixed to the moving top part (Figure 5). It is a “sensible” arrangement: camera axes are horizontal, while their angular distribution roughly balanced around the shaft of the hexapod (about

120 ° between each). Approximate pixel size with the used optical setup is 14 μm .

Machine command and DIC measurement are performed with a dedicated PC equipped with 2 GTX590 graphic boards. 900×900 pixels ZOI are used. The number of iterations is limited to 5 to keep computation time below the period between two successive images (50 ms since cameras have a 20 Hz frame rate).

4.2 Automated calibration step

First, a calibration step is performed, with an actuator length of calibration set to 150 μm . The figure 6 shows the measured 3D displacements by each of the camera during this calibration step. For the sake of clarity, only T_x , which is a “sensitive” shape function, and R_x , which is a “low sensitive” shape function, are presented. The sequence of displacement of each actuator one after the other is clearly visible. A simplistic but quick way to check if the camera arrangement is sensible (though not yet optimized) is to verify that each actuator displacement can be distinguished from the others. This is clearly shown by figure 6. Of course, the determining factor is eventually that the matrix $\sum_i C_i^{-1} M_i C_i$ in Eq. 8 has a low condition number.

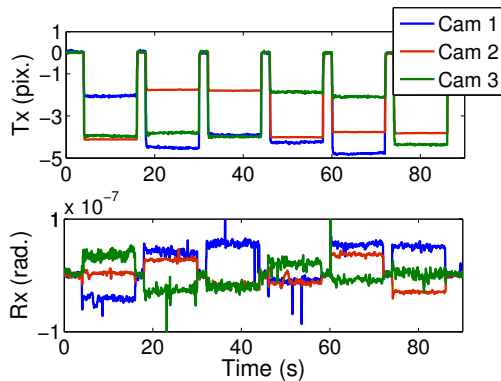


Figure 6: Two of the 3D displacements measured by each of the camera during the calibration step.

4.3 Measurement results

Once the calibration step is performed, a series of simple tests is performed. It does not yet include closed-loop control, only open-loop,

with DIC setup used as an auxiliary measurement.

The standard deviations of the measured lengths have been calculated with a 200-point sample (*i.e.* a 10 s measurement) acquired with the machine switched on and with a constant command. The standard deviation is around 0.8 μm for 4 out of the 6 actuators. Actuator 5 value is about 0.4 μm and actuator 3 value about 1.3 μm . Small vibrations of the actuators in themselves, due to the high power command, may influence this results. Moreover, low frequency components, *a priori* not due to the numerical algorithm but to the machine or the surrounding, are clearly visible during a 10 s period, especially on actuator 3. It explains its higher standard deviation.

A test of cyclic displacement along the y direction of the hexapod has then been performed without load, so that 3D displacements follow command signal with a minimum error. The set magnitude is such that actuator maximum positive length is around the calibration length (150 μm). Figure 7 shows that the length of actuator 1 is measured during the whole motion with a difference between measurement and command signal below 10 μm . Figure 8 shows this difference versus the command signal. One sees an hysteresis loop with strong discontinuities (around 15 μm) at each change of command direction, due to the clearances in the joints of the machine. The slight slope (about 2 %) may be due to hypothesis of linear relationship (*i.e.* use of calibration matrices) whereas the real geometry induces non-linear laws. One notices that the difference is not higher in the negative range ($[-150, 0]$ μm), though the calibration was limited to the positive range ($[0, +150]$ μm).

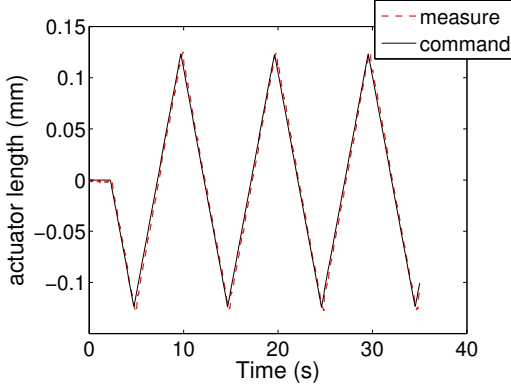


Figure 7: Comparison of measured length of actuator 1 and its command during a cyclic displacement.

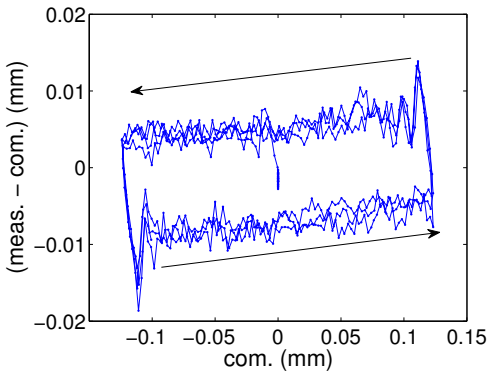


Figure 8: Difference between measure and command as a function of command. Hysteresis loop due to clearances is noticeable.

5 CONCLUSIONS

An innovative measurement technique has been developed to perform modern Nooru-Mohamed tests. First tests are very convincing even though the setup is not optimized. It has now to be thoroughly tested and integrated in the control loop of the testing machine.

The principle is to use Integrated Digital Image Correlation that directly measure the actuators lengths from the images of “targets” fixed to the moving end of the machine. To do so, the matrices and second members built to solve the DIC equation with 3D Rigid Body Motion shape functions are combined to the linear relation in between 3D RBM and actuators lengths, determined by a calibration step. The minimization is directly performed in terms of actuators lengths with redundant camera data in a

single iterative process, avoiding the measurement of 3D RBM for each camera.

The proposed method is very versatile in the sense that it may be used with any kinematic architecture and number of cameras. In the present case, a parallel architecture (hexapod) is used, with three cameras to reach the desired accuracy. The only limitation is the non-linearity of the kinematic. With the required small displacement range (around $100 \mu\text{m}$) in comparison with the size of the used hexapod (actuator length of about 1.5 m), non-linearity is not a problem for Nooru-Mohamed tests.

6 ACKNOWLEDGEMENTS

The authors want to thank Stéphane Roux for his helpful conversation and advice.

REFERENCES

- [1] Nooru-Mohamed, M.B., 1992. Mixed mode fracture of concrete: An experimental approach. Doctoral thesis. Delft University.
- [2] Nierenberger, M., Poncelet, M., Pattofatto, S., Hamouche, A., Raka, B. and Virely, J.-M. Multiaxial testing of materials using a Stewart platform: case study of the Nooru-Mohamed test, *Exp. Techn.*, in press.
- [3] A. Stokes, M. Gardner-Morse, D. Churchill and J.P. Laible (2002). *Measurement of a Spinal Motion Segment Stiffness Matrix*. Journal of Biomechanics, vol. 35, pages 517-521.
- [4] J. G. Michopoulos, J. C. Hermanson and T. Furukawa (2008). *Towards the robotic characterization of the constitutive response of composite materials*. Composite Structures, vol. 86, pages 154-164
- [5] H. Leclerc, J.-N. Périé, S. Roux, and F. Hild (2009). *Integrated Digital Image Correlation for the Identification of Material Properties*. Lecture Notes in Computer Science, volume 5496, pages 161-171.